Electronic Supplementary Material (ESI) for Journal of Materials Chemistry C.
This journal is © The Royal Society of Chemistry 2019

Integrated outstanding precision and mechanical performance transparent 3D photonic crystals devices employing cross-linked nanospheres via thermoforming under rubbery state

Dan Chen‡, Ying Yao‡, Yunming Wang*, Yue Fu, Jiaqi Zheng, Huamin Zhou

Characterization methods

The particle size distribution was measured by the zetasizer NANO ZS90 (Malvern Instruments; Malvern, UK). A JEOL (field emission scanning electron microscope (FESEM), JSM-6500F, Japan) was used to characterize the size and morphology of the particles (covered with a thin layer of gold particles). The transmission of visible light were measured by UV-vis (UV-visible) spectra by use of UV-VIS (NIR) spectrophotometer (SolidSpec-3700, Shimadzu, Japan). Photoelastic experiments were conducted to characterize the OPD value with a stress birefringence instrument (PHL WPA-100, LUCEO, Japan) using hybrid light wavelength including 523 nm, 543 nm and 575 nm. Measurement of the Fourier Transform Infrared Spectroscopy (FT-IR) spectra was performed using a Spectrum One FT-IR Spectrometer (VERTEX 70, Bruker, German) and all infrared spectra were recorded using two scans for each specimen. X-ray diffraction (XRD) results were characterized by XRD-7000 (Shimadzu, Japan) ranging from 5° to 85°. The decomposition temperature and T_g of the sample were measured using the thermogravimetric (TG) analysis (TGA, Perkin-Elmer Pyris 1, USA) to help analyze the temperature range of high elastic state. The nanoindentation tests were performed on Nano Indenter (TI750, Bruker, USA) with a static measurement mode. The atomic force microscope (AFM) measurements were carried out with a surface probe microscope TopoMetrix Explorer. Dynamic mechanic analysis (DMA) was performed on the samples of 20×5×1 mm^3 in size using a dynamic mechanical analyzer under tension mode in a temperature range of ambient to 180 °C at a frequency of 1 Hz and heatingrate of 3 °C/min (DMA Q800, TA Instruments, USA). The tensile test were conducted on electronic dynamic and static fatigue machine (E3000, Instron, Britain) at 1 mm/min test speed.

Microstructure of PC devices with different size of nanospheres

To investigate the effect of the size of nanospheres, the poly (MMA-*co*-BD-5 wt.%) nanospheres having four different diameters (160 nm, 200 nm, 230nm and 260 nm) were measured for comparison. During the polymerization process, the diameter of cross-linked nanospheres can be controlled by fine-changing amounts of emulsifier. The mean nanospheres diameter is measured by zetasizer and characterized by scanning electron microscope (SEM), and the results are shown in Fig. S1a. The 3D photonic crystal devices by assembling nanospheres with three different diameters

were fabricated under the same thermoforming condition (68 MPa, 160 ℃). The SEM photos of the top and cross-sectional view of PC devices were shown in Fig. S1b and 1c.

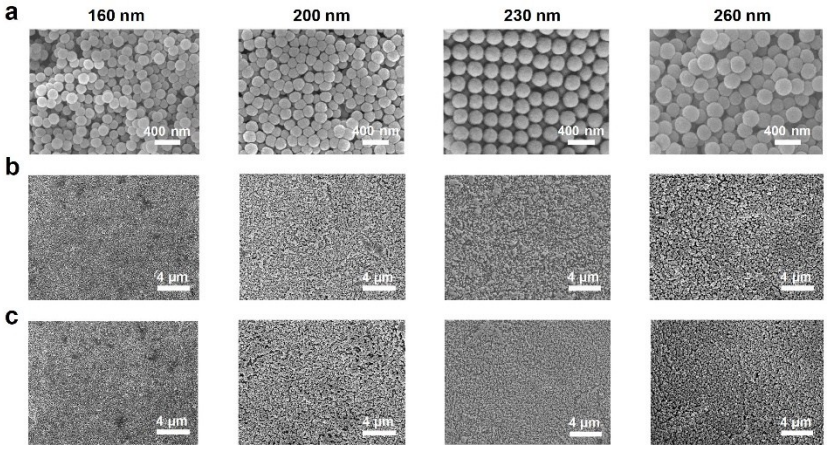

Fig. S1 SEM Photos: (a) Cross-linked PMMA nanospheres polymerized via soap-free polymerization, (b) Top view of cross-linked PMMA PC devices and (c) Cross-sectional view of cross-linked PMMA PC devices.

Properties of PC devices with different size of nanospheres

The solid fluidity of nanospheres with different sizes can be characterized by a rheometer under 1 s^{-1} shear rate (shown in Fig. S2a). At the forming temperature, the viscosity of nanospheres, whose mean size are 230 nm and 260 nm, are rather close and lower than 5 Pa.s, in contrast, the viscosity exhibited a sharp increase with the decrease of the size of nanospheres originated from the availability of the higher surface area and the formed cluster which was strong enough to resist the external shear stress. At this point, lower viscosity is prone to form uniform optical properties during the thermoforming process. Furthermore, the optical properties were characterized. The optical path difference of four PC devices was measured via a stress birefringence instrument, the optical path difference (OPD) values on the centerline of devices were extracted automatically (shown in Fig. S2b). It can be concluded that the OPD of four devices are all lower than 20 nm, however, the fluctuation of OPD of the poly (MMA-*co*-BD-5 wt.%)-160 nm and 200 nm devices is slightly higher than that of poly (MMA-*co*-BD-5 wt.%)-230 nm and 260 nm devices attributed the higher viscosity of nanospheres with smaller size. In the case of the poly (MMA-*co*-BD-5 wt.%) with four different sizes of nanospheres, the transmittance was recorded by UV-VIS (NIR) spectrophotometer ranging from 300 nm to 1000 nm (shown in Fig. S2c). At the wavelength of 760 nm, the transmittance of devices is 88.91% (160 nm), 89.21% (200 nm), 89.69% (230 nm), and 89.12% (260 nm), which poly (MMA-*co*-BD-5 wt.%) -230 nm devices exhibit a slight higher transmittance than another

three devices.

Once the devices were assembled, another challenge that needs to face is the ability to withstand external pressure. The contact stiffness, elastic modulus, and hardness were determined by the nanoindentation test. It can be seen in Fig. S2d that the hardness and modulus of poly (MMA-*co*-BD-5 wt.%) -160 nm and 200 nm devices corresponding to 5.82 ± 0.08 GPa and 0.44 ± 0.03 GPa, 5.51 ± 0.03 GPa and 0.3 ± 0.01 GPa are slightly higher than poly (MMA-*co*-BD-5 wt.%) -230 nm device corresponding to 5.71 ± 0.09 GPa and 0.32 ± 0.01 GPa. However, the stiffness of poly (MMA-*co*-BD-5 wt.%) -230 nm device is higher than other three devices.

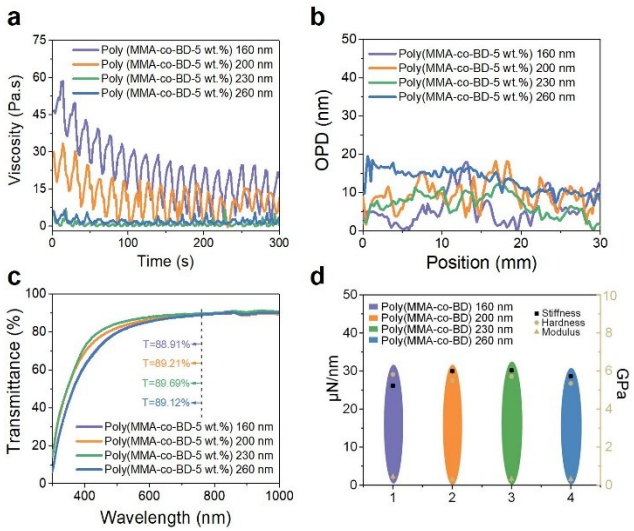

Fig. S2 (a) Solid fluidity of cross-linked PMMA nanospheres at the forming temperature (160 ℃) under the shear rate 1 s^{-1}. (b) OPD of four PC devices with different size of nanospheres. (c) Visible-light transmittance of four PC devices. (d) Nanoindentation results of four PC devices.

On the basis of the experimental results, we chose 230 nm as nanospheres' size to fabricate PC devices.

Microstructure and photos of PC devices

It is observed that the average size of cross-linked PMMA photonic crystal (PC) nanospheres were around 230 nm in SEM photos, which are monodispersed and have uniform shape. Moreover, from the photos of PMMA PC devices, it can be directly founded that the transparency towards the pattern of poly (MMA-*co*-BD) and poly (MMA-*co*-TMPTMA) devices are slight higher than poly (MMA-*co*-DVB) PC devices.

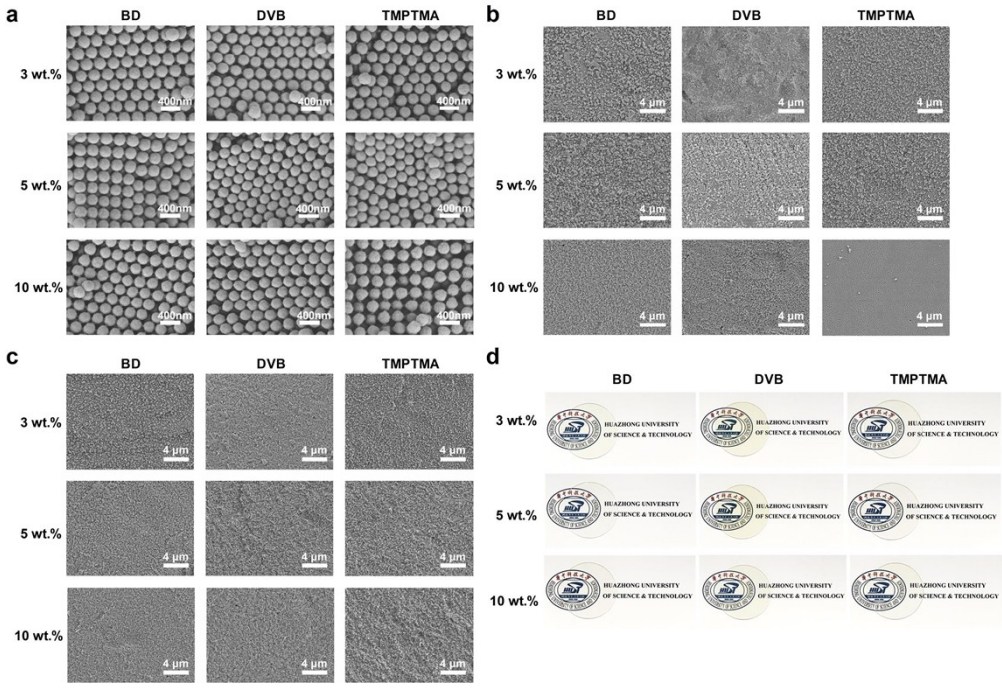

Fig. S3 SEM photos: (a) Cross-linked PMMA PC powder nanospheres, (b) Top view of cross-linked PMMA PC devices, (c) Cross-sectional view of cross-linked PMMA PC devices. (d) Sample photos.

The 3D PC can be described via Bragg's law,[1-3] as depicted in eqn (1) - (3):

$$\lambda = 2d\sqrt{n_{eff}^2 - sin^2\theta} \tag{1}$$

$$\mathrm{d} = \sqrt{2/3}D \tag{2}$$

$$n_{eff} = \sqrt{f_{sphere}n_{sphere}^2 + f_{air}n_{air}^2} \tag{3}$$

in which d is the distance between two neighboring crystalline planes in the (111) direction, which is linked to the PMMA nanospheres diameter D (= 230 nm) for the face-center cubic (fcc) structure, and its relation with the sphere diameter D is shown in eqn (2). The effective refractive index (n_{eff}) can be approximated according to eqn (3), where f_{sphere} = 0.74 is the filling ratio for the polymer in the fcc structure, n_{sphere} is 1.49, and f_{air} is 0.26, n_{air} is 1, respectively.

In the contrast results of reflectance spectrum, we can notice that the reflectance also decrease with the increase of cross-linking agents, and the trend is opposite to the relationship between transmittance and cross-linking agents, which is another side to confirm that cross-linking agents can enhance the transparency of device. The reflection peak wavelength is regulated to around 400 nm, which led to a decline of transmittance around 400 nm.

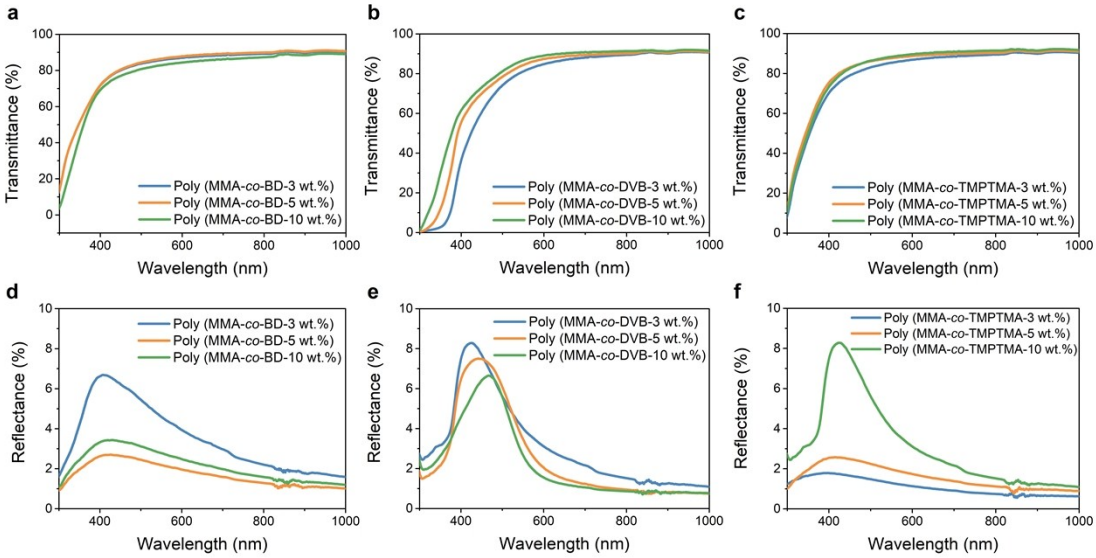

Fig. S4 The transmittance of device containing different mass percent cross-linking agents: (a) Poly (MMA-*co*-BD), (b) Poly (MMA-*co*-DVB) and (c) Poly (MMA-*co*-TMPTMA). The reflectance of device containing different mass percent cross-linking agents. (d) Poly (MMA-*co*-BD), (e) Poly (MMA-*co*-DVB) and (f) Poly (MMA-*co*-TMPTMA).

The FTIR spectra and XRD curves depicted the functional groups and amorphous state of cross-linked PMMA PC devices. With the increase of BD, $T_{5\%}$ of microspheres rises and then falls, which could be attributed to the tunable benzene ring and long side group of BD, and the poly (MMA-*co*-DVB) microspheres have the same trend with poly (MMA-*co*-BD), however, there is a difference that the temperature of poly (MMA-*co*-DVB) just changes slightly from 3 wt.% to 10 wt.% attributed to rigid benzene ring. Interestingly, with the increase of TMPTMA, the $T_{5\%}$ shows a marked rise, which can be assigned to the bulky side group of TMPTMA.

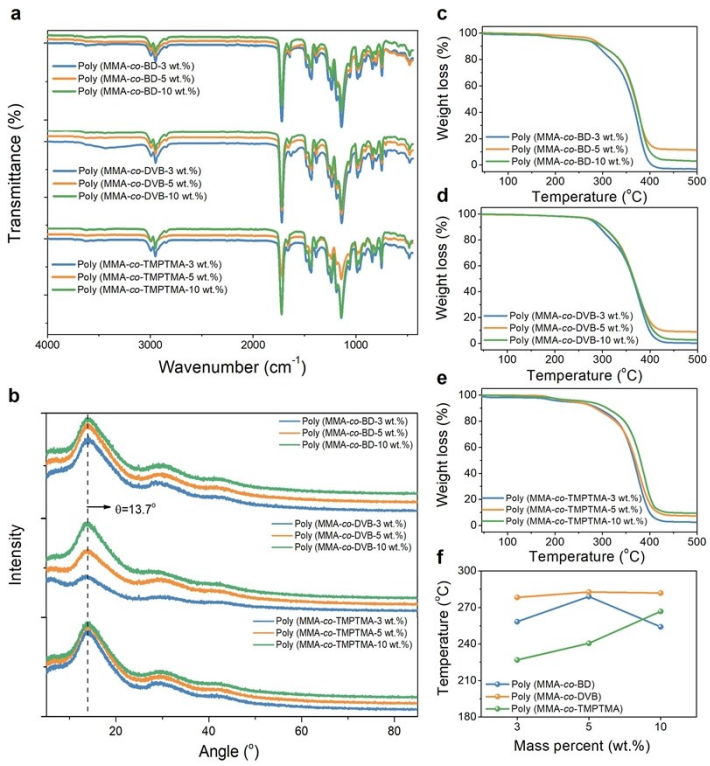

Fig. S5 (a) FTIR spectra curves of poly (MMA-*co*-BD), poly (MMA-*co*-DVB), poly (MMA-*co*-TMPTMA). (b) XRD curves. TG analysis curves: (c) Poly (MMA-*co*-BD). (d) Poly (MMA-*co*-DVB) and (e) Poly (MMA-*co*-TMPTMA). (f) The $T_{5\%}$ values recorded by TG analysis.

For poly (MMA-*co*-BD), the average contact stiffness of 3 wt.%, 5 wt.%, 10 wt.% are 31.11 ± 0.21 μN/nm, 30.16 ± 0.16 μN/nm, 30.31 ± 0.08 μN/nm, respectively. For poly (MMA-*co*-DVB), the average contact stiffness of 3 wt.%, 5 wt.%, 10 wt.% are 30.10 ± 0.23 μN/nm, 29.13 ± 0.14 μN/nm, 36.07 ± 0.13 μN/nm, respectively. For poly (MMA-*co*-TMPTMA), the average contact stiffness of 3 wt.%, 5 wt.%, 10 wt.% are 30.11 ± 0.19 μN/nm, 35.13 ± 0.47 μN/nm, 29.09 ± 0.2 μN/nm, respectively. For poly (MMA-*co*-BD), the average modulus of 3 wt.%, 5 wt.%, 10 wt.% are 5.56 ± 0.15 GPa, 5.71 ± 0.09 GPa, 5.44 ± 0.06 GPa, separately. For poly (MMA-*co*- DVB), the average modulus of 3 wt.%, 5 wt.%, 10 wt.% are 5.24 ± 0.07 GPa, 5.39 ± 0.07 GPa, 8.32 ± 0.06 GPa, separately. For poly (MMA-*co*-TMPTMA), the average modulus of 3 wt.%, 5 wt.%, 10 wt.% are 5.45 ± 0.09 GPa, 7.66 ± 0.16 GPa, 5.18 ± 0.08 GPa, separately. For poly (MMA-*co*-BD), the average hardness of 3 wt.%, 5 wt.% and 10 wt.% are 0.29 ± 0.01 GPa, 0.32 ± 0.01 GPa, 0.287 ± 0.05 GPa, respectively. For poly (MMA-*co*-DVB), the average hardness of 3 wt.%, 5 wt.%, 10 wt.% are 0.27 ± 0.01 GPa, 0.31 ± 0.01 GPa, 0.48 ± 0.07 GPa, respectively. For poly (MMA-*co*-TMPTMA), the average hardness of 3 wt.%, 5 wt.%, 10 wt.% are 0.29 ± 0.07 GPa, 0.42 ± 0.02 GPa, 0.28 ± 0.01 GPa, respectively.

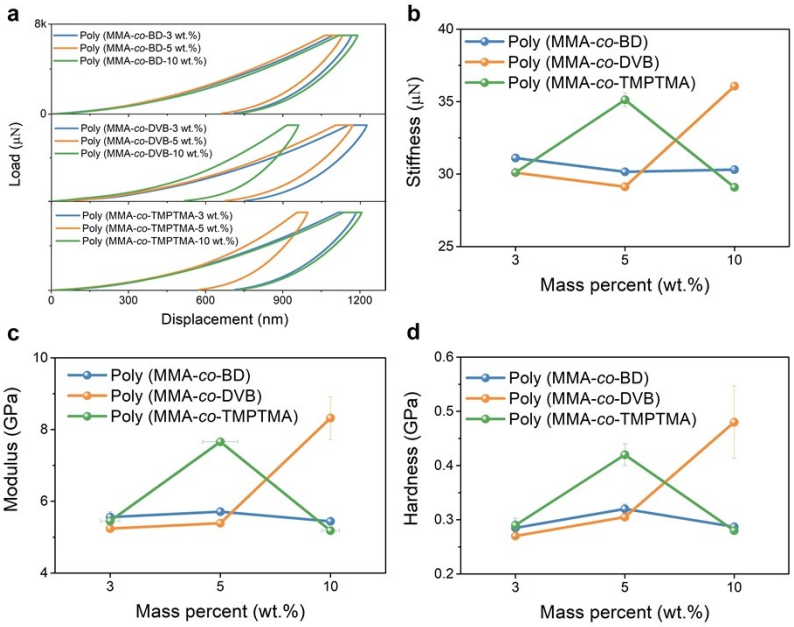

Fig. S6 Nanoindentation of cross-linked PMMA PC devices. (a) Load-depth curves (at 7000 μN applied load). (b) Contact stiffness. (c) Modulus. (d) Hardness.

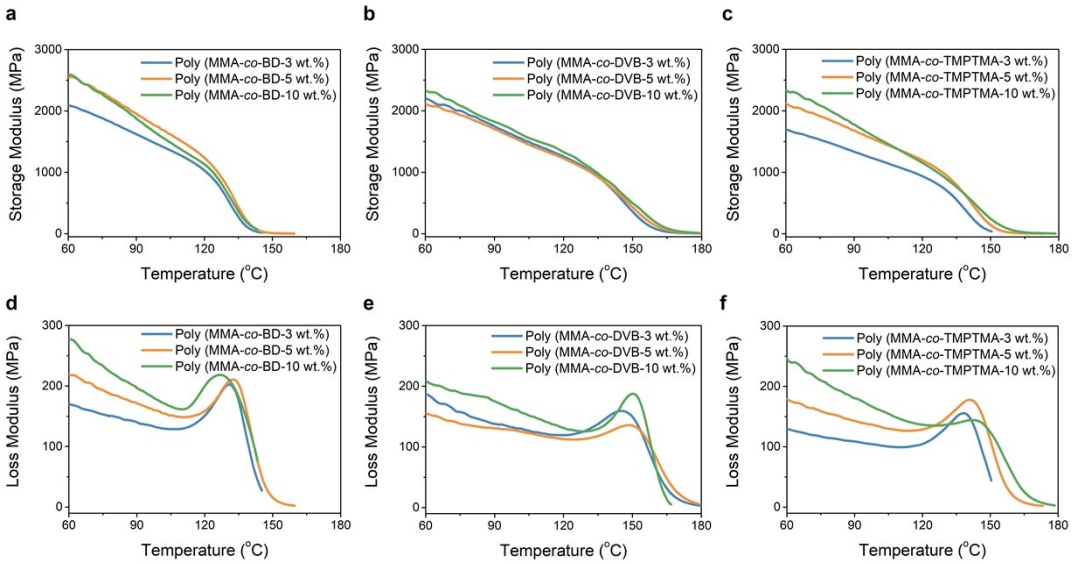

Fig. S7 The Storage modulus curves of cross-linked PMMA PC devices: (a) poly (MMA-*co*-BD) and uncross-linked PMMA sample, (b) poly (MMA-*co*-DVB) and (c) poly (MMA-*co*-TMPTMA). The loss modulus of cross-linked and uncross-linked PMMA devices: (d) poly (MMA-*co*-BD) and uncross-linked PMMA sample, (e) poly (MMA-*co*-DVB) and (f) poly (MMA-*co*-TMPTMA).

For poly (MMA-*co*-BD), the average tensile strength of 3 wt.%, 5 wt.%, 10 wt.% are 49.75 ± 3.59 MPa, 52.58 ± 7.65 MPa, 48.53 ± 6.4 MPa, separately. For poly (MMA-*co*-DVB), the average tensile strength of 3 wt.%, 5 wt.%, 10 wt.% are 19.97 ± 0.58 MPa, 21.47 ± 0.44 MPa, 20.52 ± 0.18 MPa, separately. For poly (MMA-*co*-TMPTMA), the average tensile strength of 3 wt.%, 5 wt.%, 10 wt.% are 24.19 ± 2.13 MPa, 27.7 ± 3.31 MPa, 37.46 ± 2.53 MPa, separately. For poly (MMA-*co*-BD), the average elastic modulus of 3 wt.%, 5 wt.%, 10 wt.% are 2446.75 ± 72.4 MPa, 2815.19 ±

66.95 MPa, 2796.72 ± 60.89 MPa, separately. For poly (MMA-*co*-DVB), the average elastic modulus of 3 wt.%, 5 wt.%, 10 wt.% are 2652.18 ± 60.7 MPa, 3345.63 ± 28.7 MPa, 2695.09 ± 33.1 MPa, separately. For poly (MMA-*co*-TMPTMA), the average elastic modulus of 3 wt.%, 5 wt.%, 10 wt.% are 3165.01 ± 45.04 MPa, 3355.57 ± 35.56 MPa, 2905.17 ± 2.71 MPa, separately.

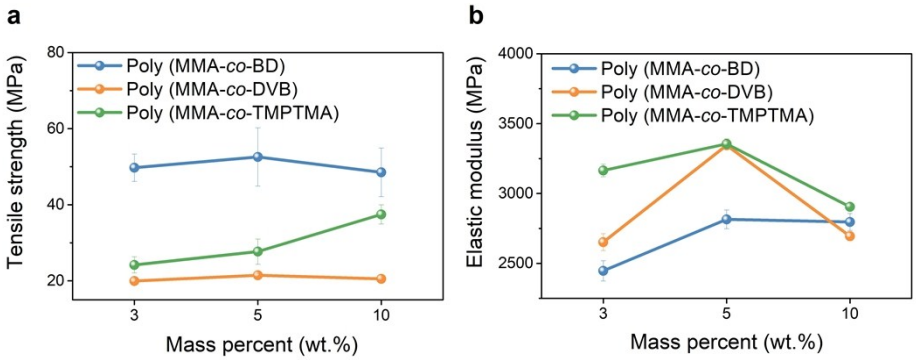

Fig. S8- The tensile test result of cross-linked PMMA PC devices: (a) Tensile strength. (b) Elastic modulus.

References

1 X. Su, H. Xia, S. Zhang, B. Tang and S. Wu, *Nanoscale*, 2017.

2 C.F. Lai and J.S. Li, *Optical Materials*, 2019.

3 M. M. Ito, A. H. Gibbons, D. T. Qin, D. Yamamoto, H. D. Jiang, D. Yamaguchi, K. Tanaka and E. Sivaniah, *Nature*, 2019, **570**, 363.